Int. J. Nano Dimens., 8 (3): 234-240, Summer 2017

ORIGINAL ARTICLE

A density functional study on the mechanical properties of metal-free two-dimensional polymer graphitic Carbon-Nitride

Shahram Ajori; Reza Ansari; Sina Malakpour*

Department of Mechanical Engineering, University of Guilan, Rasht, Iran

Received 07 February 2017; revised 25 April 2017; accepted 01 May 2017; available online 03 May 2017

Abstract

Successful synthesis of the stable metal-free two-dimensional polymer graphitic carbon-nitride with remarkable properties has made it as one of the most promising nanostructures in many novel nanodevices, especially photocatalytic ones. Understanding the mechanical properties of nanostructures is of crucial importance. Thus, this study employs density functional theory (DFT) to obtain the mechanical properties of graphene-like graphitic carbon-nitride (g-C_3N_4) nanosheets such as Young's, bulk and shear moduli and Poisson's ratio. Based on the results, Young's, bulk and shear moduli of this nanosheet are lower than those of graphene and hexagonal boron-nitride sheet. Besides, it is observed that the values of the aforementioned properties for graphene-like g-C_3N_4 nanosheets are higher than those of porous graphene and SiC. It is further observed that the Poisson's ratio of graphene-like g-C_3N_4 nanosheets is lower than those of any similar two-dimensional graphitic structures.

Keywords: *Bulk modulus; Density functional theory; Graphitic carbon-nitride; Shear modulus; Young's modulus.*

How to cite this article

Ajori Sh, Ansari R, Malakpour S. A density functional study on the mechanical properties of metal-free two-dimensional polymer graphitic Carbon-nitride. Int. J. Nano Dimens., 2017; 8 (3): 234-240.

INTRODUCTION

The fascinating properties of two-dimensional nanosheets with single atomic thickness enable researchers to design and fabricate various novel nanodevices [1-16]. Since the exfoliation of graphene, many efforts have been put into the characterizing different organic and inorganic two-dimensional nanosheets such as other graphene allotropes (graphane, graphyne, etc), porous graphene, hexagonal boron-nitride, Molybdenum disulfide and so on due to their intriguing properties and considerable potential applications in nanoelectromechanical systems (NEMS). Among the various fabricated nanomaterials, carbon nanostructures such as graphene and its allotropes and boron carbon nitride nanostructures (BCN) have been the focus of interest [17-24]. Predicting the properties of different phases of carbon nitride is demonstrated that β-C_3N_4 possesses noticeably high bulk modulus which is comparable to that of diamond. This property has motivated the researchers to explore the properties of phases of dense C_3N_4. Experimentally, different techniques have been employed to synthesize the theoretically predicted phases of C_3N_4 [25-27]. As the physiochemical properties of any phases and allotropes of nanomaterials are different from those of their two-dimensional structures due to quantum confinement effects in the sub-nanometer scales [28-30], studying their properties is of considerable importance in material science and engineering. Considering C_3N_4, it is found that its graphitic allotropes (g-C_3N_4) are the most stable allotropes with hexagonal structure which have strong C-N covalent bonds instead of C-C ones with small pores on the sheets. G-C_3N_4 can be fabricated through different methods such as solvothermal synthesis, mechanochemical reactions, thermal decomposition and so on [31-36]. Based on the published literature, several investigations on this metal-free semiconductor graphene-like polymer with medium band gap compared to the zero band gap of graphene, together with its great thermal and chemical stability and remarkable optical and

* Corresponding Author Email: *shahram_ajori1366@yahoo.com*

photoelectrochemical properties [37, 38] make it the most suitable material with considerably promising applications such as catalysts [39-41], lithium ion storages [42], optoelectronics [43-44], bioimaging and biomedical applications [45].

Determination the mechanical properties of nanostructures are of high importance. To the best of the author's knowledge, the mechanical properties of g-C_3N_4 nanosheets have not been investigated so far. Motivated by this issue, this study is performed to investigate the mechanical properties such as Young's, bulk and shear moduli and Poisson's ratio of g-C_3N_4 nanosheets employing density functional calculations (DFT).

EXPERIMENTAL

To perform DFT calculations, the Quantum-Espresso code [46] with the exchange correlation of Perdew-Burke-Ernzerhof (PBE) throgh GGA frameworks [47-48] is employed. Moreover, Brillouin zone integration is taken with a Monkhorst-Pack [49] k-point mesh of 12 × 12× 1 and the value of cut-off energy for plane wave expansion is chosen to be 80 Ry. As the results are not sensitive to unit cell dimension, the smallest hexagonal unit cell is selected and appropriate loading conditions are applied and the strain energies are stored. Finally, using the second derivative of strain energy with respect to the applied strain [50-51], the elastic constants such as Young's, bulk and shear moduli are computed. Poisson's ratio is also calculated. Note that the equations corresponding to the calculation of the elastic constants are described in the following sections.

RESULTS AND DISCUSSION

In order to achieve a better understanding of graphene-like g-C_3N_4 nanosheets, Fig. 1 is presented. This figure demonstrates the hexagonal unit cell and the values of lattice constants, i.e. and which indicate the first and second lattice constants after structural optimization process, respectively. As shown, the unit cell has three carbon atoms and four nitrogen atoms which are indicated by gray and blue colors, respectively. The optimized structure is imposed by appropriate loadings.

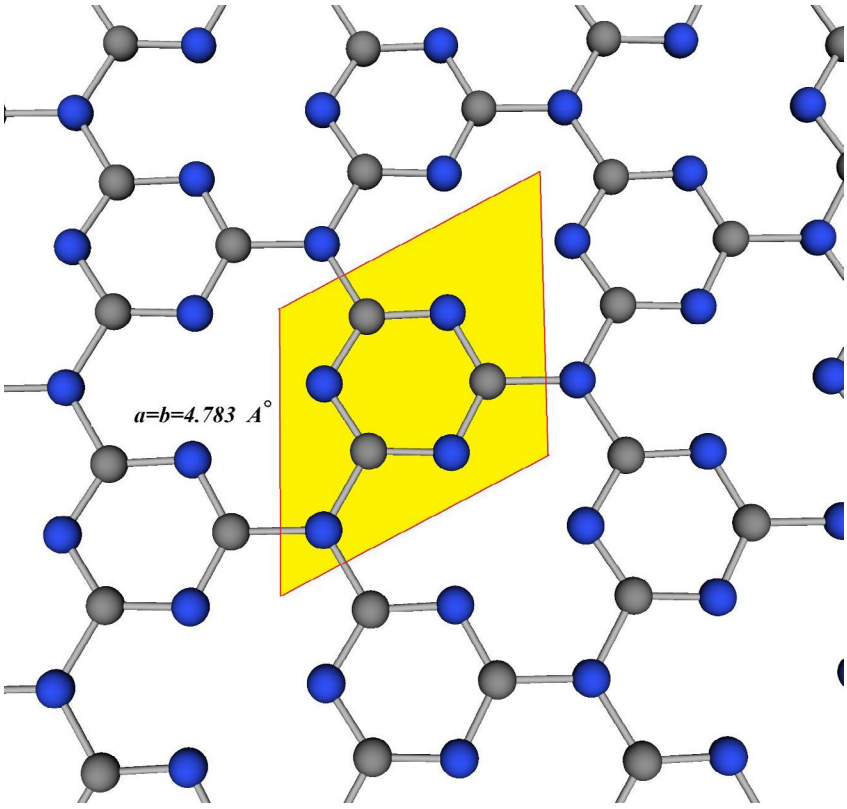

Fig. 1: Unit cell of graphene-like g-C_3N_4.

Young's modulus and Poisson's ratio

In order to compute Young's modulus, the uniaxial strains in the harmonic elastic range, *i.e.* -2% to 2%, are applied to the unit cell as illustrated in Fig. 2 and the strain energies related to the applied strains are computed.

By fitting a polynomial of second degree to data sets, Young's modulus is calculated through performing the second derivative of strain energy with respect to the applied strain according to Eq. (1).

$$Y_s = (1/A_0) \times (\partial^2 E_S / \partial \varepsilon^2) \quad (1)$$

in which A_σ, E_s and ε indicate the equilibrium optimized area of hexagonal unit cell, strain energy and axial strain, respectively. The calculations show that Young's modulus of graphene-like g-C_3N_4 nanosheets is around 238.5 *Pa.m* which is almost 29% and 11% lower than those of graphene [13] and hexagonal boron-nitride [13] nanosheets, respectively. Additionally, it is found that the stiffness of graphene-like g-C_3N_4 nanosheets is around 1.9 and 1.4 times higher than those of porous graphene (PG) [16] and SiC [13-15] nanosheets. To make a qualitative comparison, Fig. 3 is illustrated.

Considering the Poisson's ratio, which can be computed by the ratio of the transverse strain to the axial one, i.e. $\Delta a/a$ and $\Delta b/b$ for axial and transverse strains, respectively, the value of Poisson's ratio is obtained around 0.12 which is approximately 25%, 43% and 58% lower than those of graphene [13], hexagonal boron-nitride [13] and SiC [13, 15], respectively. Moreover, Fig. 4 is presented to make a graphical comparison between different values of Poisson's ratio.

Bulk modulus

To obtain the bulk modulus, biaxial strain is imposed in the harmonic elastic range as presented in Fig. 5. The bulk modulus can be also

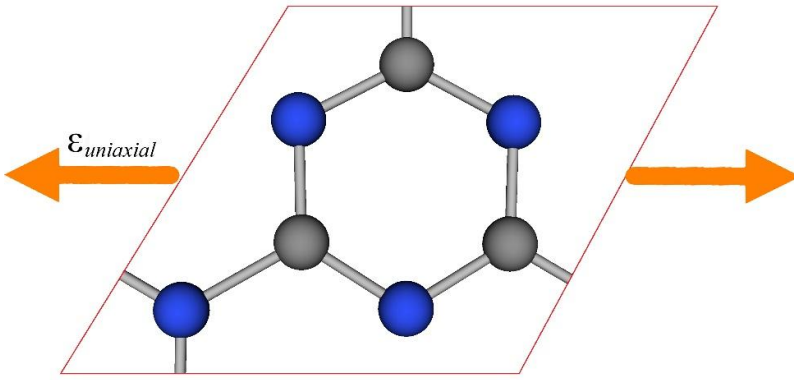

Fig. 2: Schematic representation of imposing uniaxial strain.

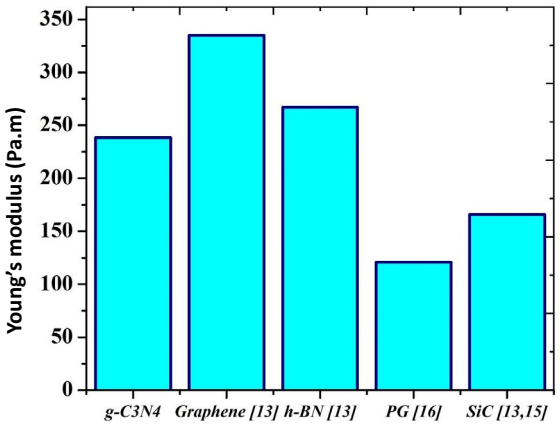

Fig. 3: Comparing Young's modulus of graphene-like g-C_3N_4 with those of other graphitic two-dimensional nanosheets.

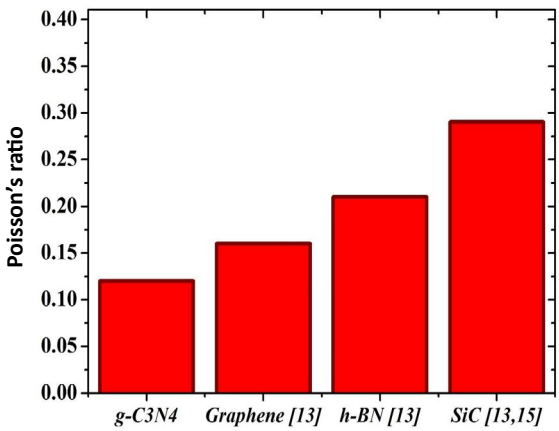

Fig. 4: Comparing Poisson's ratio of graphene-like g-C_3N_4 with those of other graphitic two-dimensional nanosheets.

obtained by fitting a polynomial of second degree to data sets and performing the second derivative of strain energy with respect to the area [12] as follows

$$B = A \times (\partial^2 E_S / \partial A^2) \quad (2)$$

where A shows the area of unitcell during deformation. It is observed that the bulk modulus of graphene-like g-C_3N_4 nanosheets is around 122.6 Pa.m which is 39% and 23.3% lower than those of graphene [12] and hexagonal boron-nitride nanosheets [12], respectively. Such a discrepancy is shown in Fig. 5.

Shear modulus

Shear modulus of two-dimensional nanosheets can be obtained by imposing shear strain according to Fig. 6. Furthermore, a similar process related to Young's modulus is utilized to compute the shear modulus [5] by Eq. (3).

$$B = \frac{1}{A_0} \times (\partial^2 E_S / \partial \gamma_{xy}^2) \quad (3)$$

in which γ_{xy} presents the shear strain. Based on the results, the shear modulus of graphene-like g-C_{34} nanosheets is calculated around 121.93 Pa.m. According to the published literature, different values for the shear modulus have been reported varying from ~121 [11] to ~138 Pa.m [10]. Comparing the results shows that the shear modulus of graphene-like g-C_3N_4 nanosheets is close to that of graphene in comparison with other elastic constants. The highest percentage of discrepancy between the existing data is around 11.5%. It is also found that the shear modulus of graphene-like g-C_3N_4 nanosheets is 26% lower than that of hexagonal boron-nitride [14]. Finally, Figs. 7 and 8 is illustrated to make a comparison between the values of shear modulus reported in the literature.

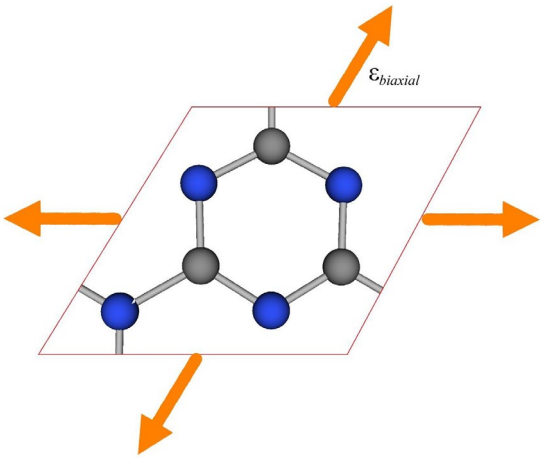

Fig. 5: Schematic representation of imposing biaxial strain.

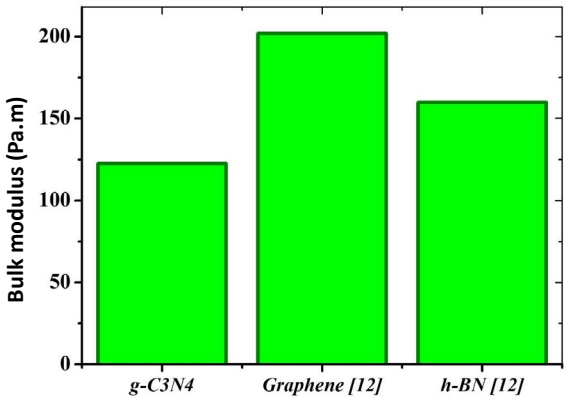

Fig. 6: Comparing the bulk modulus of graphene-like g-C_3N_4 with those of other graphitic two-dimensional nanosheets.

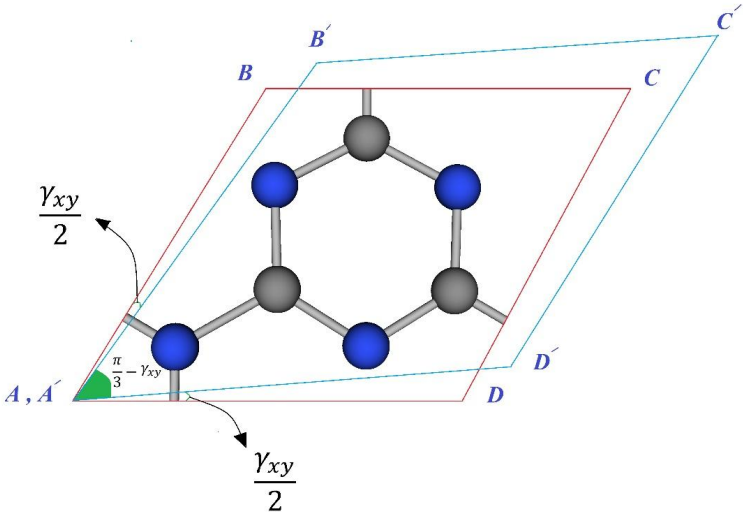

Fig. 7: Schematic representation of imposing shear strain.

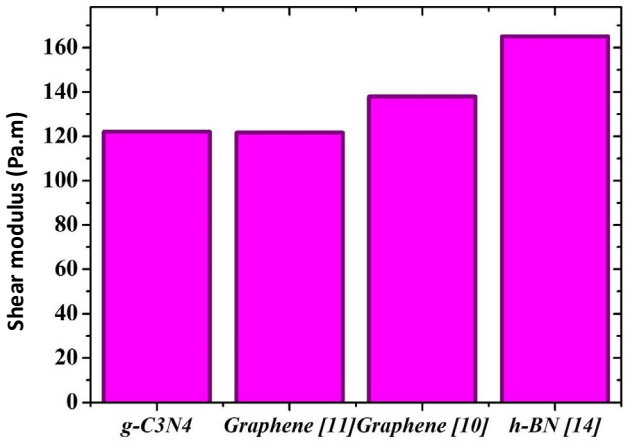

Fig. 8: Comparing the shear modulus of graphene-like g-C_3N_4 with those of other graphitic two-dimensional nanosheets.

CONCLUSION

Based on the DFT calculations, Young's, bulk and shear moduli and Poisson's ratio of graphene-like g-C_3N_4 nanosheet, a metal-free two-dimensional polymer graphitic carbon-nitride, were investigated. The obtained results demonstrated that this structure possesses lower Young's, bulk and shear moduli compared to graphene and hexagonal boron-nitride. On the contrary, it was found that the values of the aforementioned constants for graphene-like g-C_3N_4 nanosheets are higher than those of porous graphene and SiC nanosheets. Considering the Poisson's ratio, it was further observed that graphene-like g-C_3N_4 nanosheets have smaller Poisson's ratios compared to those of other two-dimensional graphitic nanosheets.

CONFLICT OF INTEREST

The authors declare that there is no conflict of interests regarding the publication of this manuscript.

REFERENCES

[1]. Novoselov K. S., Geim A. K., Morozov S. V., Jiang D., Zhang Y., Dubonos S. V., Firsov A. A., (2004), Electric field effect in atomically thin carbon films. *Science.* 306: 666-669.

[2]. Simchi H., Esmaeilzadeh M., Mazidabadi H., (2013), The electronic transport properties of porous zigzag graphene clusters. *Physica E: Low-Dimens. Systems and Nanostruc.* 54: 220-225.

[3]. Ansari R., Ajori S., Motevalli B., (2012), Mechanical properties of defective single-layered graphene sheets via molecular dynamics simulation. *Superlat. Microstruc.* 51: 274-289.

[4]. Ansari R., Motevalli B., Montazeri A., Ajori S., (2011), Fracture analysis of monolayer graphene sheets with double vacancy defects via MD simulation. *Solid State Communications.* 151: 1141-1146.

[5]. Ansari R., Malakpour S., Faghihnasiri M., Ajori S., (2013), Characterization of the mechanical properties of monolayer molybdenum disulfide nanosheets using first principles. *J. Nanotechnol. Engineer. Medicine.* 4: 034501-034507.

[6]. Splendiani A., Sun L., Zhang Y., Li T., Kim J., Chim C. Y., Wang F., (2010), Emerging photoluminescence in monolayer MoS_2. *Nano Letters.* 10: 1271-1275.

[7]. Ansari R., Ajori S. Malakpour S., (2016), Characterization of elastic properties of porous graphene using an Ab Initio Study. *J. Ultrafine Grained Nanostruct. Mater.* 49: 97-102.

[8]. Ouyang T., Chen Y., Xie Y., Yang K., Bao Z., Zhong J., (2010), Thermal transport in hexagonal boron nitride nanoribbons. *Nanotechnol.* 21: 245701-245708.

[9]. Ajori S., Ansari R., (2014), Torsional buckling behavior of boron-nitride nanotubes using molecular dynamics simulations. *Current Appl. Phys.* 14: 1072-1077.

[10]. Min K., Aluru N. R., (2011), Mechanical properties of graphene under shear deformation. *Appl. Phys. Lett.* 98: 013113-013117.

[11]. Ansari R., Ajori S., Malakpour S., (2016), Prediction of structural and mechanical properties of atom-decorated porous graphene via density functional calculations. *The Europ. Phys. J. Appl. Phys*. 74: 10401-10406.

[12]. Nag A., Raidongia K., Hembram K. P., Datta R., Waghmare U. V., Rao C. N. R., (2010), Graphene analogues of BN: Novel synthesis and properties. *ACS Nano.* 4: 1539-1544.

[13]. Topsakal M., Cahangirov S., Ciraci S., (2010), The response of mechanical and electronic properties of graphane to the elastic strain. *Appl. Phys. Lett.* 96: 091912-091918.

[14]. Verma V., Jindal V. K., Dharamvir K., (2007), Elastic moduli of a boron nitride nanotube. *Nanotechnol*. 18: 435711-435718.

[15]. Bekaroglu E., Topsakal M., Cahangirov S., Ciraci S., (2010), First-principles study of defects and adatoms in silicon carbide honeycomb structures. *Physic. Rev. B.* 81: 075433-075439.

[16]. Jungthawan S., Reunchan P., Limpijumnong S., (2013), Theoretical study of strained porous graphene structures and their gas separation properties. *Carbon.* 54: 359-364.

[17]. Civalek O., Akgöz B. (2013), Vibration analysis of micro-scaled sector shaped graphene surrounded by an elastic matrix. *Comp. Mater. Sci.* 77: 295-303.

[18]. Zhao S., Xue J., (2013), Mechanical properties of hybrid graphene and hexagonal boron nitride sheets as revealed by molecular dynamic simulations. *J. Phys. D: Appl. Phys.* 46: 135303-135309.

[19]. Akgöz B., Civalek O., (2015), A microstructure-dependent sinusoidal plate model based on the strain gradient elasticity theory. *Acta Mechanica.* 226: 2277-2294.

[20]. Mercan K, Civalek O., (2016), DSC method for buckling analysis of boron nitride nanotube (BNNT) surrounded by an elastic matrix. *Compos. Struc*. 143: 300-309.

[21]. Lee C. G, Wei X. D., Kysar J. W., Hone J., (2008), Measurement of the elastic properties and intrinsic strength of monolayer graphene. *Science*. 321: 385–388.

[22]. Zhi C. Y., Bando Y., Tang C. C., Huang Q., Golberg D., (2008), Boron nitride nanotubes: Functionalization and composites. *J. Mater. Chem.* 18: 3900-3908.

[23]. Radisavljevic B., Radenovic A., Brivio J., Giacometti I. V., Kis A., (2011), Single-layer MoS_2 transistors. *Nature Nanotechnol.* 6: 147-150.

[24]. Mak K. F., Lee C., Hone J., Shaz J., Heinz T. F., (2010), Atomically thin MoS_2: A new direct-gap semiconductor. *Phys. Rev. Lett.* 105: 136805-136809.

[25]. Reunchan P., Jhi S. H., (2011), Metal-dispersed porous graphene for hydrogen storage. *Appl. Phys. Let.* 98: 093103-093109.

[26]. Premkumar T., Geckeler K. E. (2012), Graphene–DNA hybrid materials: Assembly, applications, and prospects. *Progress in Polym. Sci.* 37: 515-529.

[27]. Li X., Wang H., Robinson J. T., Sanchez H., Diankov G., Dai H., (2009), Simultaneous nitrogen doping and reduction of graphene oxide. *J. Am. Chem. Soc.* 131: 15939-15944.

[28]. Li X., Cai W., An J., Kim S., Nah J., Yang D., Banerjee S. K., (2009), Large-area synthesis of high-quality and uniform graphene films on copper foils. *Science.* 324: 1312-1314.

[29]. Zhang Y., Tang T. T., Girit C., Hao Z., Martin M. C., Zettl A., Wang F., (2009), Direct observation of a widely tunable bandgap in bilayer graphene. *Nature.* 459: 820-823.

[30]. Kroke E., Schwarz M., (2004), Novel group 14 nitrides. *Coordinat. Chem. Rev.* 248: 493-532.

[31]. Goglio G., Foy D., Demazeau G., (2008), State of art and recent trends in bulk carbon nitrides synthesis. *Mater. Sci. Eng: Reports.* 58: 195-227.

[32]. Horvath-Bordon E., Riedel R., Zerr A., McMillan P. F., Auffermann G., Prots Y., Kroll P., (2006), High-pressure chemistry of nitride-based materials. *Chem. Soc. Rev.* 35: 987-1014.

[33]. Omomo Y., Sasaki T., Wang L., Watanabe M., (2003), Redoxable nanosheet crystallites of MnO_2 derived via delamination of a layered manganese oxide. *J. Am. Chem. Soc.* 125: 3568-3575.

[34]. Ithurria S., Tessier M. D., Mahler B., Lobo R. P. S M., Dubertret B., Efros A. L., (2011), Colloidal nanoplatelets with two-dimensional electronic structure. *Nature Mater.* 10: 936-941.

[35]. Geim A. K., Novoselov K. S., (2007), The rise of graphene. *Nature Mater.* 6: 183-191.

[36]. Li C., Yang X., Yang B., Yan Y., Qian Y., (2007), Synthesis and characterization of nitrogen-rich graphitic carbon nitride. *Mater. Chem. Phys.* 103: 427-432.

[37]. Bojdys M. J., Müller J. O., Antonietti M., Thomas A., (2008), Ionothermal synthesis of crystalline, condensed, graphitic carbon nitride. *Chem: A. Europ. J.* 14: 8177-8182.

[38]. Zhen-Yi F., Yu-Xian L., (2003), Effective route to graphitic carbon nitride from ball-milled amorphous carbon in NH_3 atmosphere under annealing. *Chinese Phys. Let.* 20: 1554-1561.

[39]. Zhao H., Chen X., Jia C., Zhou T., Qu X., Jian J., Zhou T., (2005), A facile mechanochemical way to prepare gC_3N_4. *Mater. Sci. Engineer: B.* 122: 90-93.

[40]. Goglio G., Foy D., Pechev S., Majimel J., Demazeau G., Guignot N., Andrault D., (2009), Evidence for a low-compressibility carbon nitride polymorph elaborated at ambient pressure and mild temperature. *Diam. Related Mater.* 18: 627-631.

[41]. Jürgens B., Irran E., Senker J., Kroll P., Müller H., Schnick W., (2003). Melem (2, 5, 8-Triamino-tri-s-triazine), an important intermediate during condensation of melamine rings to graphitic carbon nitride: Synthesis, structure determination by X-ray powder diffractometry, solid-state NMR and theoretical studies. *J. Am. Chem. Soc.* 125: 10288-10300.

[42]. Wang X., Maeda K., Thomas A., Takanabe K., Xin G., Carlsson J. M., Antonietti M., (2009), A metal-free polymeric photocatalyst for hydrogen production from water under

visible light. *Nature Mater.* 8: 76-80.
[43]. Wang Y., Wang X., Antonietti M., (2012), Polymeric graphitic carbon nitride as a heterogeneous organocatalyst: From photochemistry to multipurpose catalysis to sustainable chemistry. *Angewa. Chemie. Int. Edition.* 51: 68-89.
[44]. Niu P., Liu G., Cheng H. M. (2012), Nitrogen vacancy-promoted photocatalytic activity of graphitic carbon nitride. *J. Phys. Chem. C.* 116: 11013-11018.
[45]. Wang Y., Hong J., Zhang W., Xu R., (2013), Carbon nitride nanosheets for photocatalytic hydrogen evolution: Remarkably enhanced activity by dye sensitization. *Catalysis Sci. Technol.* 3: 1703-1711.
[46]. Yan H., Chen Y., Xu S., (2012), Synthesis of graphitic carbon nitride by directly heating sulfuric acid treated melamine for enhanced photocatalytic H_2 production from water under visible light. *Int. J. Hydrogen Energy.* 37: 125-133.
[47]. Fang Y., Lv Y., Che R., Wu H., Zhang X., Gu D., Zhao D., (2013), Two-dimensional mesoporous carbon nanosheets and their derived graphene nanosheets: synthesis and efficient lithium ion storage. *J. Am. Chem. Soc.* 135: 1524-1530.
[48]. Zhang Y., Mori T., Niu L., Ye J., (2011), Non-covalent doping of graphitic carbon nitride polymer with graphene: controlled electronic structure and enhanced optoelectronic conversion. *Energy & Environ. Sci.* 4: 4517-4521.
[49]. Zhang Y., Mori T., Ye J., Antonietti M., (2010), Phosphorus-doped carbon nitride solid: enhanced electrical conductivity and photocurrent generation. *J. Am. Chem. Soc.* 132: 6294-6295.
[50]. Zhang X., Xie X., Wang H., Zhang J., Pan B., Xie Y., (2012), Enhanced photoresponsive ultrathin graphitic-phase C_3N_4 nanosheets for bioimaging. *J. Am. Chem. Soc.* 135: 18-21.
[51]. Baroni S., Corso D. A., Gironcoli S., Giannozzi P., Cavazzoni C., Ballabio G., Scandolo S., Chiarotti G., Focher P., Pasquarello A., Laasonen K., Trave A., Car R., Marzari N., Kokalj A., *http://www.pwscf.org/.*
[52]. Perdew J. P., Burke K., Ernzerhof M., (1996), Generalized gradient approximation made simple. *Phys. Rev. Lett.* 77: 3865-3871.
[53]. Perdew J. P., Burke K., Wang Y., (1998), Erratum: Generalized gradient approximation for the exchange-correlation hole of a many-electron system. *Phys. Rev. B.* 57: 14999-15008.
[54]. Monkhorst H. J., Pack J. D., (1976), Special points for Brillouin-zone integrations. *Phys. Rev. B.* 13: 5188-5196.
[55]. Wagner P., Ivanovskaya V. V., Rayson M. J., Briddon P. R., Ewels C. P., (2013), Mechanical properties of nanosheets and nanotubes investigated using a new geometry independent volume definition. *J. Phys: Condens. Matt.* 25: 155302-155309.
[56]. Zhukovskii Y. F., Piskunov S., Pugno N., Berzina B., Trinkler L., Bellucci S., (2009), Ab initio simulations on the atomic and electronic structure of single-walled BN nanotubes and nanoarches. *J. Phys. Chem. Solids.* 70: 796-803.